NEWLIT – A General Code for Neutron Wall Loading Distribution

H. Attaya and M. Sawan

February 1985

UWFDM-629

Presented at the Sixth Topical Meeting on the Technology of Fusion Energy, San Francisco, CA, 3-7 March 1985; Fusion Tech. 8, (July 1985).

FUSION TECHNOLOGY INSTITUTE

UNIVERSITY OF WISCONSIN

MADISON WISCONSIN

NEWLIT – A General Code for Neutron Wall Loading Distribution

H. Attaya and M. Sawan

Fusion Technology Institute
University of Wisconsin
1500 Engineering Drive
Madison, WI 53706

http://fti.neep.wisc.edu

February 1985

UWFDM-629

Presented at the Sixth Topical Meeting on the Technology of Fusion Energy, San Francisco, CA, 3-7 March 1985; Fusion Tech. 8, (July 1985).

NEWLIT - A GENERAL CODE FOR NEUTRON WALL LOADING DISTRIBUTION IN TOROIDAL REACTORS

HOSNY M. ATTAYA and MOHAMED E. SAWAN
Fusion Technology Institute, University of Wisconsin
1500 Johnson Drive, Madison, WI 53706
(608) 263-6398 or (608) 263-5093

ABSTRACT

A computer program for evaluating the poloidal distribution of the neutron wall loading (NWL) in toroidal fusion reactors is developed using numerical integration for general plasma and wall shapes. The neutron source within the plasma could be uniform or could be described to properly represent the neutron density associated with the magnetic flux surfaces. The method and techniques used in NEWLIT are presented. A comparison with the Monte-Carlo code MCNP shows excellent agreement with substantial savings in computer time and required user time. To verify the validity of the NWL as calculated by NEWLIT, a detailed 3-D neutronics calculation was carried out for a representative tokamak reactor. The poloidal distribution of the important responses is compared to the NWL poloidal distribution.

INTRODUCTION

The neutron wall loading (NWL) is an important parameter usually used to estimate the lifetime of the first wall (FW) of fusion reactors. There is considerable deviation, at different locations of a tokamak FW, from the nominal value of the NWL (defined as the neutron fusion power divided by the FW surface area). This deviation should be taken into account for any reliable estimate of the FW lifetime, and must be identified for proper design of the FW. The NWL distribution in test facilities is also important as it indicates where materials test modules, blanket test modules, and plasma neutronic diagnostics devices should be located to utilize the neutron source values needed to accomplish the mission of the facility. Any response function, at any location in the reactor, depends on the the materials used and the original neutron source. There is no doubt that the nuclear response functions depend on the plasma neutron source, and consequently the poloidal variation of the response functions depends on the poloidal variation of the plasma neutron source. This is verified in the last section of this paper.

The NWL distribution can be determined using Monte Carlo codes,[1] which due to their statistical nature require large computer times to achieve reasonable accuracy. However, these codes are the only choice to handle complicated geometries. Dänner[2] was the first to calculate the NWL in toroidal geometries using a deterministic method. To achieve that the first wall and the plasma were assumed circular with uniform source density. The angular flux at a point on the wall was related to the active length of the ray in the direction of the angular flux. This active length, which is the part (or parts) of the ray that lies within the source, was evaluated by iteration or by solving a fourth order algebraic equation. Price and Chapin[3] used explicit tracing of the ray to evaluate the angular flux for nonuniform sources and circular cross section tokamaks. They extended this explicit ray-tracing to noncircular cross section tokamaks.[4]

In the above two methods, the total uncollided flux could be evaluated by integrating the angular flux. The neutron current crossing the wall (NWL) could be evaluated in the same way taking into account the direction of the normal to the wall. It is clear that to achieve high accuracy for the NWL or the flux, a large number of rays should be traced, and this is required for each wall point, implying large computer time that could be comparable to that required for solving the problem by Monte Carlo codes. In this paper, we present the computer program NEWLIT (NEutron Wall Load In Torus) that uses a simpler method to calculate the poloidal distribution of the uncollided neutron current (NWL) and flux in toroidal reactors for general plasma and wall shapes.

METHOD

The neutron current J at a point w on the wall is given by

$$J = \int_V \frac{S(\bar{R}_p)}{4\pi|\bar{R}_w-\bar{R}_p|^2} \frac{(\bar{R}_w-\bar{R}_p)}{|\bar{R}_w-\bar{R}_p|} \cdot \bar{n}_w dV \qquad (1)$$

where $S(\bar{R}_p)$ is the neutron source at $\bar{R}_p$ and is assumed isotropic, $\bar{R}_w$ is the position vector for w, $\bar{n}_w$ is the unit normal to the wall at w, and the integration is over the part V of the plasma which produces neutrons that can directly reach w. Using the cylindrical coordinate components of $\bar{R}_p(r_p,\theta,z_p)$ and $\bar{R}_w(r_w,0,z_w)$, Eq. 1 can be rewritten as

$$J = \iiint \frac{S(r_p,z_p)[(r_w-r_p\cos\theta)n_x+(z_w-z_p)n_z]r_p dr_p d\theta dz_p}{4\pi \left| r_w^2 - 2r_p r_w\cos\theta + r_p^2 + (z_w-z_p)^2 \right|^{3/2}} \quad (2)$$

where n_x and n_z are the x and y components of $\bar{n}_w$. Notice that the source as well as the wall are assumed toroidally symmetric. Using this notation the uncollided neutron flux at w is given by:

$$\Phi = \iiint \frac{S(r_p,z_p)\, r_p dr_p d\theta dz_p}{4\pi\{r_w^2-2r_p r_w\cos\theta+r_p^2+(z_w-z_p)^2\}}. \quad (3)$$

Eqs. 2 and 3 are integrated numerically by dividing the source into disks (i.e z-grid) and in the case of a nonuniform source, each disk is divided into radial elements. Each element is weighted by the plasma density on the magnetic flux surface that passes through its center. The r-limits of the integration are functions of z_p, and the θ-limits are calculated from the lines of intersection of the plane $Z=z_p$ with all the tangent planes to the inboard surfaces between z_w and z_p, and are passing through the point w, as explained below.

Consider a torus the cross section of which is shown in Fig. 1a. The inboard surfaces S_1 (cone) and S_2 (cylinder) are generated by the generatrices AB and BC respectively. Consider also a source disk a-b and a point W on the wall. It is required now to determine the part of the disk a-b that can be seen from W. This part is limited by the tangent planes to S_1 and S_2 that pass through W. The tangent plane to S_1 intersects the plane $Z=z_w$ in a circle of radius R_1, determined by substituting z_w in the equation of the generatrix AB. The tangent line to this circle from W at the plane $Z=z_w$ ($W-T_1$ in Fig. 1b) lies also in the tangent plane and is parallel to all the intersection lines of the tangent plane with any horizontal plane. The equation of the line $W-T_1$ as shown in Fig. 1b is

$$x\cos(\phi_j) + y\sin(\phi_j) - R_j = 0,\ j=1 \quad (4)$$

where j refers to the surface number, and ϕ_1 is the angle of the perpendicular to $W-T_1$ ($o-T_1$) and is equal to

$$\phi_j = \cos^{-1}(R_j/r_w),\ j=1\ . \quad (5)$$

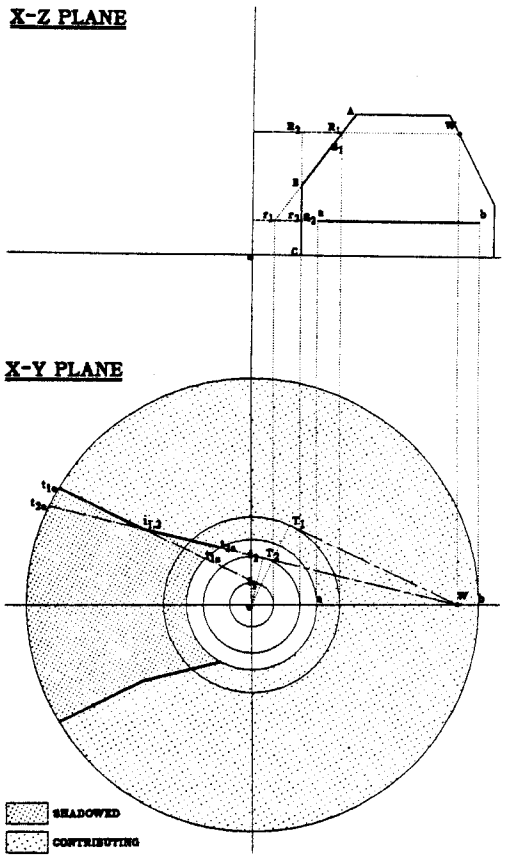

Fig. 1. (a) X-Z cross section showing the wall point W with respect to source disk a-b; (b) X-Y view showing contributing and shadowed parts of the source disk.

The equation of the intersection line of the tangent plane with the plane $Z=z_p$ can be determined in the same way, and is

$$x\cos(\phi_j) + y\sin(\phi_j) - r_j = 0,\ j=1 \quad (6)$$

where r_j (j=1) is the radius of the circle resulting from the intersection of S_1 with the $Z=z_p$ plane. This line intersects the two circles r=a and r=b at the points t_{1s} and t_{1e}. If S_1 is the only inboard surface between z_w and z_p, the line t_{1s}-t_{1e} will be the boundary of the part of the disk that can be seen from W. In this case the required toroidal limit as can be seen from Fig. 1b varies from

$$\theta_{j1} = \cos^{-1}(r_j/a) + \phi_j,\ j=1 \quad (7)$$

to

$$\theta_{j2} = \cos^{-1}(r_j/b) + \phi_j,\ j=1 \quad (8)$$

as r varies from a to b.

The same steps are repeated for the surface S_2, and similar equations (Eqs. 5 to 8 with j=2) are obtained. Each line t_{js}-t_{je} (with j=1, 2 in this example) separates the shadowed and unshadowed parts of the disk due to the surface S_j. The net contributing part of the source disk a-b to the NWL or the flux will be bounded by these lines. This boundary starts with the line which gives the minimum value of θ_1 and ends with the line that gives the minimum value of θ_2. The intersection point of two consecutive lines gives an intermediate point on that boundary. Thus in the example shown in Fig. 1, the integration limits of θ are

$$\theta = \cos^{-1}(r_2/r) + \phi_2 \quad r_{i1,2} > r > a \qquad (9)$$

and

$$\theta = \cos^{-1}(r_1/r) + \phi_1 \quad b > r > r_{i1,2} \qquad (10)$$

where $r_{i1,2}$ is the radius of the intersection point of the lines t_{1s}-t_{1e} and t_{2s}-t_{2e}. This procedure can be carried out for any number of inboard surfaces between any point on the wall and any source disk and the integration of Eqs. 2 and 3 is straightforward.

The first wall boundary can be input to NEWLIT, or can be generated internally by specifying the ratio of the wall radius to the plasma radius. This allows the evaluation of the neutron current very close to the plasma itself. The source boundary can be input also, or can be calculated from the parametric equations of the D-shaped plasma[5] (also used for circular plasma), or from the parametric equations of the bean-shaped plasma.[6] In the case of the circular and D-shaped plasma, the neutron source can be peaked and shifted from the minor axis. More details about the method and these parametric equations are given elsewhere.[7]

COMPARISON WITH MONTE CARLO CALCULATIONS

Fig. 2 shows a schematic of the FW cross section and the NWL distribution in INTOR. Also shown are the contours of the magnetic flux surfaces, and the neutron source distribution at the midplane. The NEWLIT results are compared to those of the Monte Carlo code MCNP[1] in Fig 3. Half a million histories were used in MCNP to yield less than 1% statistical uncertainty. An estimate of the error in the NEWLIT results was made by integrating the computed NWL over the FW surface; the error was less than .1%. The MCNP and NEWLIT results are in excellent agreement, but the striking difference was in the computer time. The MCNP calculations used 3.4 minutes of CRAY computer CPU time, compared to only 2 seconds consumed by NEWLIT. Only a few minutes are needed to prepare the NEWLIT input, which is substantially less than the time required, for an experienced MCNP user, to prepare the input,

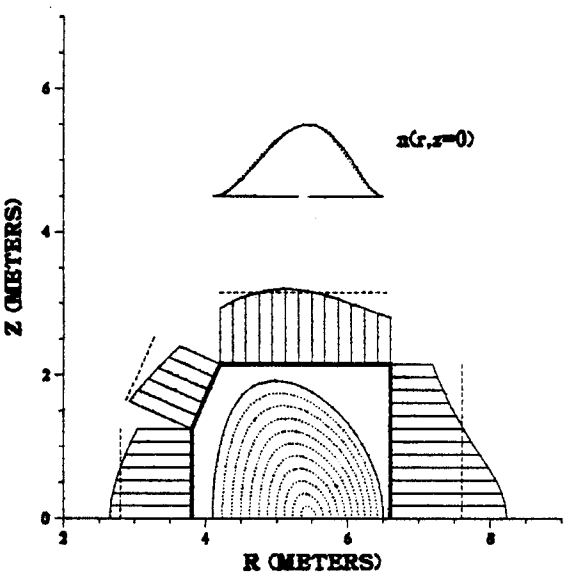

Fig. 2. Cross section of INTOR.

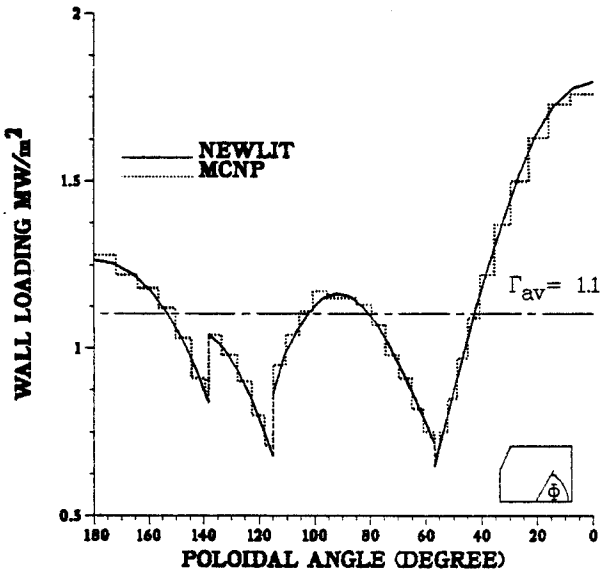

Fig. 3. Comparison of the NWL calculated by NEWLIT and by MCNP.

write the source routine, compile and load MCNP, and finally to execute it. It is also important to mention that the size of computer memory required for NEWLIT is considerably less than that

required for MCNP.

APPLICATIONS

There are many interesting features of the poloidal distribution of the current and flux in toroidal geometries. In this section we present examples that serve also to illustrate the different outputs of NEWLIT.

In the first example, the NWL and flux distributions of a bean-shaped plasma are calculated and compared to those of a D-shaped plasma of equivalent power. In the second example we show the effect of the aspect ratio on the HWL and flux in STARFIRE. Figure 4 shows a bean shaped plasma and a D-shaped plasma. The powers of both sources were adjusted to give the nominal NWL value of 1 MW/m^2. Both sources are assumed uniform. The current and flux of the bean source are compared to those of the D-shape in Fig. 5. The flux and current of the bean shape are reduced by a factor of ~ 30% from that of the D-shape at the inboard leg of the FW while they slightly increased in the other zones. The sharpness of the peak and the shift of non-uniform bean sources are more pronounced than those of non-uniform D-shaped sources (e.g. Fig. 2). This would account for higher reduction in the NWL and flux as predicted from these uniform sources. Thus the use of bean-shaped plasmas results in relaxing the inboard shield thickness required to protect the toroidal field coils. This in turn would lower the maximum field in those magnets. Figure 6 shows the current to flux ratio of each case. This ratio is the average cosine of the angle of incidence with respect to the wall normal. It is clear that the neutrons incident on the outboard wall are less peaked in the bean shape case. This results in less penetration and lower radiation effects in the back zones.

Figure 7 shows a cross section STARFIRE, a schematic of the NWL, and the neutron source distribution at the midplane. The nominal value of the NWL is 3.6 MW/m^2 and the major radius R is 7 m. Figure 8 shows the NWL and flux distributions for R = 7, 20, 100, 200 m, with fixed minor radius and average NWL. As R increases from 7 m to 200 m the peak NWL decreases by ~ 15%, while the minimum NWL increases as R increases. If the flux in each case is plotted relative to its respective average value the aspect ratio effect is less pronounced than that for the NWL. The calculations were repeated for a uniform source. In this case the relative poloidal changes of the NWL and flux are less than the previous case. The peak flux shifts to the inboard side, and the peak NWL is at a poloidal angle of ~ 60°. Hence using uniform sources in neutronics calculations might lead misleading results.

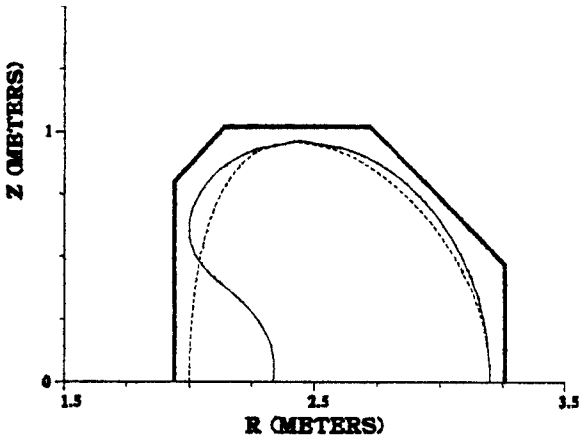

Fig. 4. Bean and D-shaped sources.

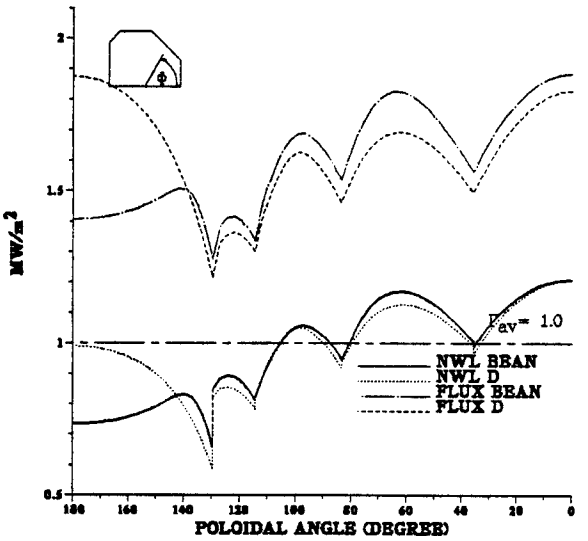

Fig. 5. The NWL and flux for the bean and D sources.

RELATION BETWEEN NWL AND NUCLEAR RESPONSES

The NWL measures the uncollided neutron current at the first wall. Secondary neutrons and gamma photons are produced by neutron interactions with the reactor materials. The collided flux component as well as the important nuclear response functions, such as radiation damage, nuclear heating, and tritium breeding, depend therefore on the geometry and materials used. To show how the NWL poloidal distribution

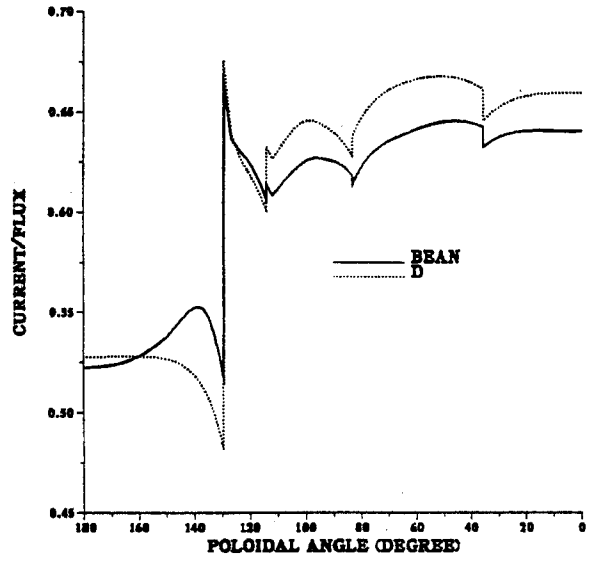

Fig. 6. The NWL to flux ratio.

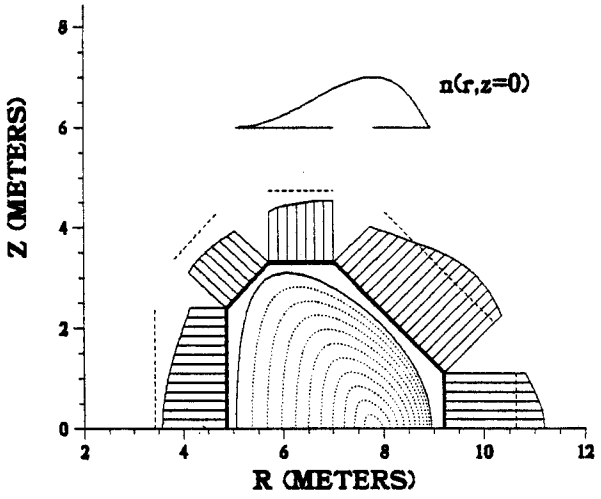

Fig. 7. Cross section view of STARFIRE.

is related to the poloidal variation of these response functions, we performed a detailed three-dimensional (3-D) neutronics calculation for a representative tokamak reactor.

A high wall loading (HWL) tokamak reactor, with a major radius of 2.6 m, an aspect ratio of 4.33 and a fusion power of 1000 MW, was modeled for MCNP calculations. The geometrical model is given in Fig. 9. A 1 cm thick HT-9 first wall is followed by two 30 cm thick blanket

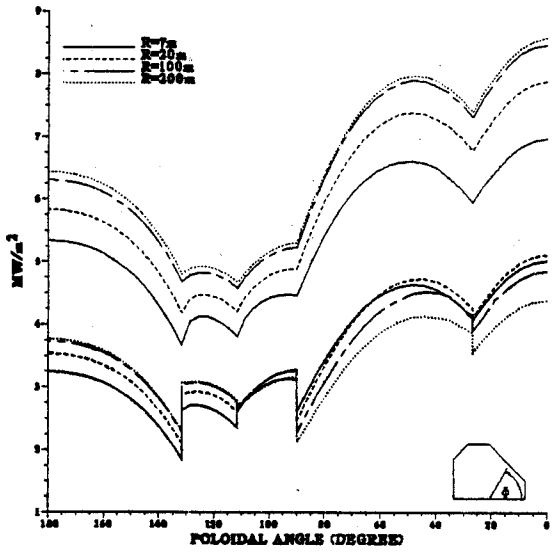

Fig. 8. The NWL (lower curves) and flux (upper curves) for different major radii.

zones made of 70 vol% $Li_{17}Pb_{83}$ (90% ^{6}Li) and 10 vol% HT-9. A 30 cm thick reflector/shield consisting of 90 vol% Fe 1422 and 10 vol% H_2O was used. The zones were segmented into 39 poloidal segments using conical surfaces that go through the plasma minor axis. 30,000 histories were used in the calculation that took 10 hours of CPU time on the CRAY computer yielding responses averaged over the segment volumes. Statistical uncertainties of 1-10% and 5-50% were obtained in the front and back zones, respectively. A separate calculation, in which no materials were used, gave the poloidal variation of the NWL accurate to ~ 0.5% with million histories used.

The poloidal variation of the nuclear response functions in the different zones was determined. The results for the dpa rate are given in Fig. 10 and compared to the NWL distribution. The poloidal variations have the same general shape of the NWL distribution with peaks and minima occuring in the same poloidal regions. The peaking factor increases as one goes deeper in the blanket. The lower minima in the back zones are related to the fact that the corner segments are effectively at larger distances from the plasma than other segments. The inboard peak values start to exceed the outboard peaks as one moves deep in the blanket due to the enhanced contribution from neutrons impinging on adjacent areas of the inboard first wall.

We performed one-dimensional (1-D) toroidal and poloidal cylindrical geometry calculations for the HWL design considered here. The results

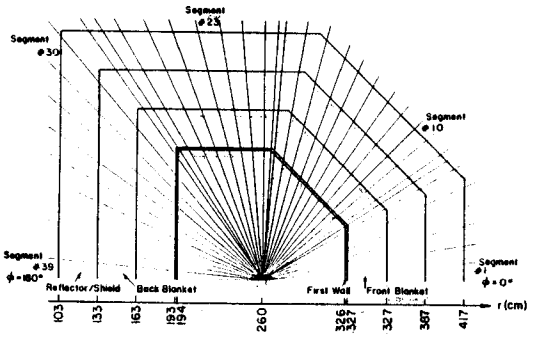

Fig. 9. Calculation model for the HWL reactor.

were coupled to the poloidal NWL variation and compared to the three-dimensional results. We found that using the calculated NWL, at the poloidal locations corresponding to hot spots in the outboard, top and bottom blankets coupled with the poloidal cylindrical 1-D results yields responses higher than the 3-D results by a factor of less than 1.2 with the overestimate being smaller in the back zones. In most cases this overestimate is within the statistical uncertainty of the 3-D results. To get a conservative estimate for radiation effects at the hot spots on the inboard side, one needs to couple the calculated NWL with the results of the toroidal cylindrical 1-D calculation in which the inboard and outboard blankets are modeled separately. In this case the overestimate is less than 60%.

It is concluded from these results that the poloidal NWL variation obtained from NEWLIT can be used to determine the poloidal zones where reactor hot spots occur. The results can then be coupled with the results of the appropriate 1-D calculation to determine the peak radiation effects. This approach is considerably less expensive and more accurate than performing a 3-D calculation in which the statistical uncertainties are large. This approach is most useful when local quantities, such as the peak damage in the magnet, are needed.

SUMMARY

A simple inexpensive code, NEWLIT, was developed to determine the neutron wall loading poloidal variation in toroidal reactors with general plasma and wall shapes. The NEWLIT results are in excellent agreement with the Monte Carlo results with order of magnitude savings in computer time. The NEWLIT results can be used to determine the poloidal zones where reactor hot spots occur. The results can then be coupled with the appropriate 1-D calculations to yield the peak radiation effects.

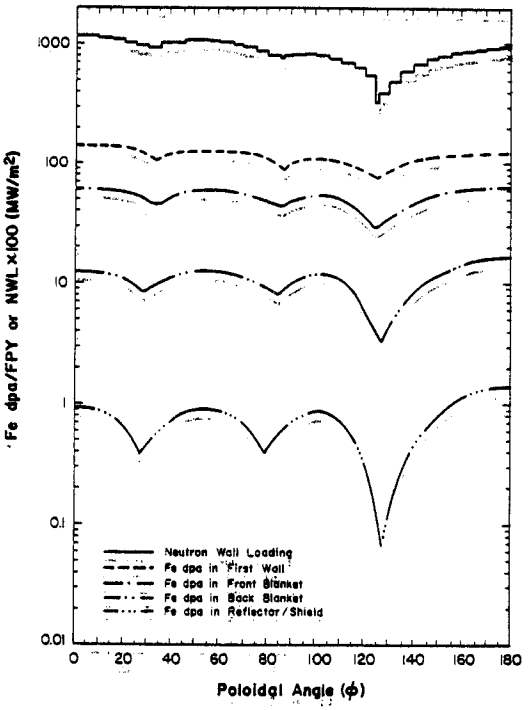

Fig. 10. Poloidal variation of dpa rate and NWL.

REFERENCES

1. "MCNP, A General Monte Carlo Code for Neutron and Photon Transport," LA-7396-M, Los Alamos National Laboratory (1981).

2. W. DÄNNER, "Neutron Flux Asymmetry in Toroidal Geometries," IPP 4/101, Max-Planck Institut für Plasmaphysik (1972).

3. W.G. PRICE, Jr. and D.L. CHAPIN, "Neutron Wall Loading Distributions in a Circular Cross Section Tokamak," MATT-1102, Princeton Plasma Physics Laboratory (1975).

4. D.L. CHAPIN and W.G. PRICE, Jr., Nuc. Tech., 31, 32 (1976).

5. K.A. VERSCHUUR, "Furnace Calculations for JET Neutron Diagnostics," ECN-146, Netherlands Energy Research Foundation (1983).

6. M.S. CHANCE, S.C. JARDIN, and T.H. STIX, Phy. Rev. Let., 51, 1963 (1983).

7. H. ATTAYA, "NEWLIT User Manual," to be published.